CrossMark

Dynamic modelling of aqueous two-phase systems to quantify the impact of bioprocess design, operation and variability

Nehal Patel [a,b], Daniel G. Bracewell [a], Eva Sorensen [b,]*

[a] *Department of Biochemical Engineering, University College London, Bernard Katz Building, Gordon Street, London, WC1E 6BT, UK*
[b] *Department of Chemical Engineering, University College London, Torrington Place, London, WC1E 7JE, UK*

ABSTRACT

Aqueous two-phase extraction (ATPE) is a promising downstream separation technology as an alternative, or addition, to chromatography in the production of biological products. Increasing demand for therapeutic proteins have triggered manufacturers to consider continuous upstream technologies to achieve greater process efficiencies; however, such technologies have an inherent variability, resulting in output streams of varying compositions and properties. It is therefore important to understand how this variability impacts on the downstream separation processes.

Exploring all potential sources of variability is challenging due to resource and time constraints, however, the use of targeted mathematical modelling can significantly reduce the need for expensive and time consuming experimentation. In this work, we present a dynamic equilibrium stage process model, and a methodology for prediction of key process parameters from limited experiments, capable of describing ATPE separations under both multi-cycle batch and continuous counter-current modes of operation. The capabilities of the proposed methodology are demonstrated using a case study separation of the enzyme α-amylase from impurities in a PEG 4000–phosphate aqueous two phase system (ATPS) containing NaCl. The model can be used to predict the separation performance of the process, as well as for the investigation of suitable design and operating conditions.

1. Introduction

The market for therapeutic proteins is currently increasing at a remarkable pace (Ecker et al., 2015). To cope with the increasing product and patient demands, drug developers are looking to take advantage of continuous manufacturing technologies for greater efficiencies. A continuous process needs to consistently produce product of a high quality throughout its entire period of operation, and regardless of process disturbances and changes. This is, however, a difficult task to achieve as the biological complexity of the cells used in upstream culture/fermentation is inherently variable. For instance, Valente et al.

(2015) recently showed that as Chinese hamster ovary (CHO) cells age, the profile of hard to remove host cell proteins (e.g. impurities with similar separation behaviour to the product) changes. In addition to such inherent variability, other sources of disturbances must also be evaluated, such as equipment failure, human error, contamination etc. Understanding the impact of process changes on whole bioprocess performance is important as product quality could be compromised if the process is not sufficiently robust. Unfortunately, it is often costly and time consuming to evaluate all sources of variability experimentally. One solution to this issue is to use predictive process models to simulate the behaviour of systems under varying conditions, such as

Nomenclature

Notation

$\beta_{i,i}$	Binary interaction parameter between component i and component i ($kg\,mol^{-1}$)
$\beta_{i,j}$	Binary interaction parameter between component i and component j where $i \neq j$ ($kg\,mol^{-1}$)
μ_i	Chemical potential of component i ($J\,mol^{-1}$)
i	Component index
$C_{i,q,n}$	Concentration of component i in stream number q in stage n ($kg\,m^{-3}$) where q is top or bottom
$\rho_{q,n}$	Density in q in stage n ($kg\,m^{-3}$) where q is top or bottom
R	Gas constant ($J\,mol^{-1}\,k^{-1}$)
$F_{q,n}$	Mass flow of stream q in stage n ($kg\,s^{-1}$) where q is stream 1–4
$x_{i,q,n}$	Mass fraction of i in q in stage n where q is either top, bottom, overall or stream 1–4
$M_{i,q,n}$	Mass holdup of i in q in stage n where q is overall, top or bottom (kg)
m_i	Molality of component i ($mol\,kg^{-1}$)
V_3	Molar volume of water ($m^3\,mol^{-1}$)
NC	Number of components
NS	Number of stages
$K_{impurities,n}$	Partition coefficient of impurities in stage n
$K_{\alpha-amylase,n}$	Partition coefficient of α-amylase in stage n
$\emptyset_n$	Phase ratio in stage n
n	Stage index
μ_1^0	Standard chemical potential of i ($J\,mol^{-1}$)
q	Location index i.e. top, bottom, overall or stream 1–4
T	Temperature (K)
$w_{i,q,n}$	Weight percent of component i in q in stage n where q is overall, top or bottom (wt%)

used in the chemical process industries for tasks such as troubleshooting, design, optimisation etc. (Chen and Mathias, 2002; Biegler and Grossmann, 2004; Klatt and Marquardt, 2009; Hendriks et al., 2010; Mathias, 2014).

ATPE is a promising alternative technology to the chromatographic technologies normally used for the separation of proteins in biopharmaceutical processing (Rito-Palomares, 2004; Soares et al., 2015). ATPE is a liquid–liquid extraction technology where two phases are formed when either two hydrophilic polymers, or a polymer and a salt, are mixed together in the presence of water above a critical concentration. Proteins and other solutes partition between the two phases based on their thermo-physical properties (Asenjo and Andrews, 2011).

Soares et al. (2015) recently conducted a SWOT (strengths, weaknesses, opportunities and threats) analysis of ATPE. A key weakness identified was the lack of predictive design, as well as expertise, in validation and operation of such two-phase processes. This weakness can be partly addressed by effective process models, but only if thermodynamic behaviour is captured adequately. Thermodynamic models allow for properties, such as densities and equilibrium phase compositions, to be determined without the need to perform extra experiments, provided thermodynamic model parameters are accurate. Often, these parameters are derived from experimental phase equilibria data using parameter estimation protocols. The application of thermodynamics to describe the non-ideal ATPS phase equilibria has been summarised well by Cabezas (1996), however, there are more recent advances, such as the use of ePC-SAFT equations of state (Reschke et al., 2014). Thermodynamic models used for ATPS phase equilibria calculations often ignore the contributions of complex proteins due to the complexity in representing large biomolecules. Empirical correlations describing protein partitioning for such systems therefore have to be obtained partly from experimental data to ensure the required model accuracy. Unfortunately, the use of detailed thermodynamics in process models used to simulate the ATPS processes has, to the best of our knowledge, so far not been considered in the literature.

Secondly, and of equal importance, the dynamic behaviour of a system must be taken into account in order to consider process variability and disturbances. Such issues are important when attempting to understand and control continuous processes which operate for long periods of time. To date, process modelling of ATPSs has been limited mainly to continuous steady-state systems (Mündges et al., 2015; Prinz et al., 2014; Samatou et al., 2007; Huenupi et al., 1999; Mistry et al., 1996). Although the dynamics of continuous operation for control of such continuous systems has been investigated by Simon and Gautam (2004), their study resulted in a system description which was not uniquely defined (−2 degrees of freedom) and where phase equilibria was characterised by empirical relationships.

To tackle these issues, we present an approach based on a dynamic stage-by-stage equilibrium model that can be used to simulate ATPE processes under a variety of configurations and operating policies. Liquid–liquid equilibria data available from literature is used to estimate interaction parameters for the thermodynamic equations used in the process model. The approach permits a fast, yet systematic, investigation of both process design and process operation for the separation of biomolecules using ATPE. The approach is demonstrated by considering dynamic continuous counter-current, as well as multi-cycle batch, modes of operation for a case study involving the separation of enzyme α-amylase from impurities in a PEG 4000–phosphate ATPS in the presence of NaCl. The level of modelling detail is deliberately kept low, partly to reduce the complexity of the equation system and partly due to the limited availability of experimental data from literature, however, we discuss in detail how the level of modelling complexity can be increased.

2. Mathematical methods

The modelling approach used in this work is illustrated in Fig. 1. A general single stage dynamic equilibrium process model is used to describe both the multi-cycle batch and the counter-current mode of operation as the fundamental physical and chemical behaviour is the same in each mode. The system consists of a number of components: (1) those characterising the two phases, either two hydrophilic polymers, or a polymer and a salt, together with water, and (2) the desired protein and other biological material (in the following denoted impurities) from the upstream fermentation stage. Chemical potential is used to describe the phase equilibria between the two aqueous phases and the thermodynamic parameters required are obtained from experimental data. Empirical correlations are used to represent the more complex behaviour of protein partitioning, as currently no thermodynamic prediction methods exist which can accurately describe this behaviour. The use of correlations to describe the behaviour of the protein and that of the impurity reduces the complexity in describing the system when considering mixtures composed of a single desired protein product plus many impurities, as is often the case when dealing with primary recovery after cell culture/fermentation. The overall equation system is solved simultaneously using gPROMS ModelBuilder 4.1 (Process Systems Enterprise, 2017).

2.1. Assumptions

In developing the process model, a number of assumptions had to be made. Most of these assumptions are similar to those
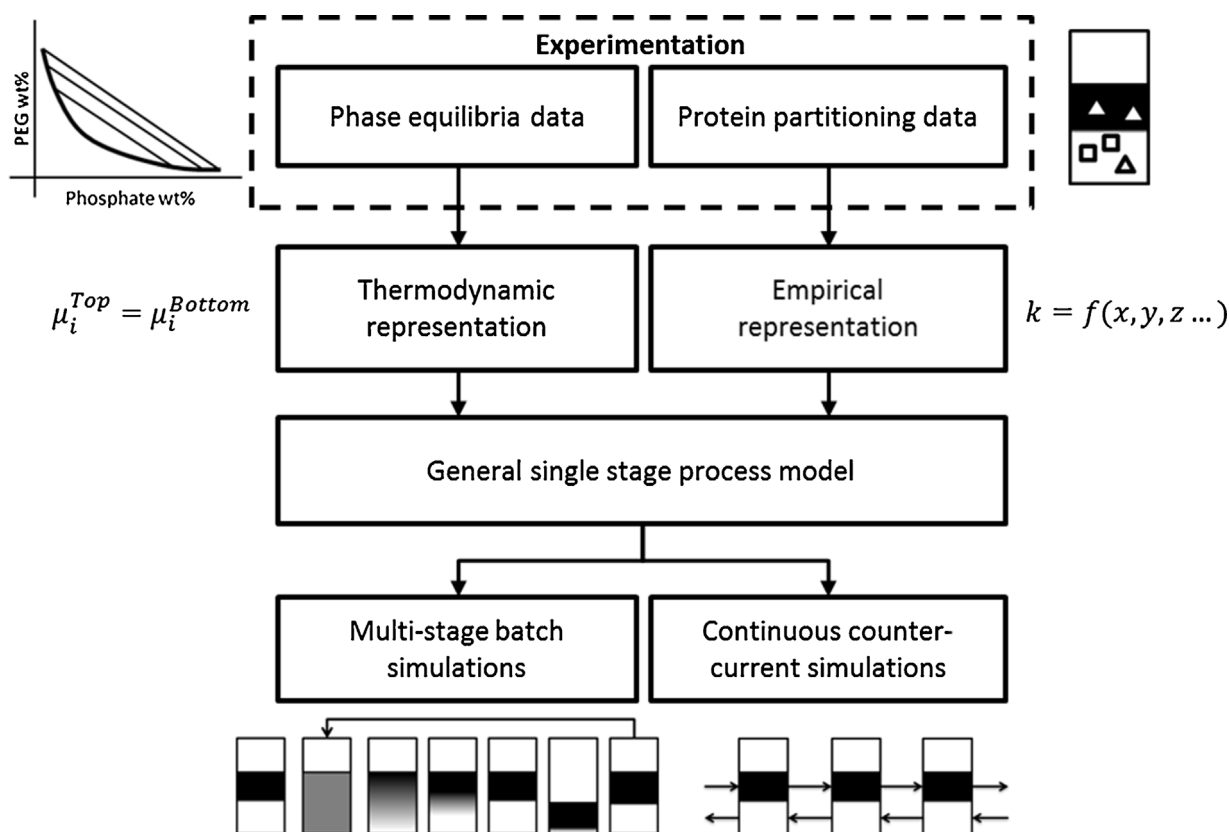
Fig. 1 – Overview of modelling framework. Experimental data is represented mathematically using appropriate equations.

made when considering other stage-wise separation methods such as distillation or absorption. The key assumptions were:

1. An energy balance was not considered as the process is considered to be isothermal (Rosa et al., 2009; Mistry et al., 1996).
2. Impurities were treated as a single component with a lumped partition coefficient. In reality, each impurity would have its own partition coefficient, however, it would be very difficult, and very time consuming, to determine all these experimentally. Also, knowing their detailed behaviour is not necessary for most investigations.
3. It was assumed that equilibrium is reached instantly in each stage and for all components, i.e. each stage is 100% efficient. This assumption is reasonable for the multi-cycle batch model where in reality one would mix the phases thoroughly and then wait for them to settle. For the continuous counter-current model, the assumption of 100% stage efficiency is not realistic since equilibrium may not be reached in each stage due to the counter-current movement. However, as for other stage-wise processes such as distillation and absorption, the assumption of 100% efficiency can be made and combined with an appropriate stage efficiency. For instance, a 20 stage system with a 50% stage efficiency can be described as a 10 stage equilibrium system (Don and Robert, 2008). (Note that the stage efficiency would need to be determined experimentally.)
4. It was assumed that the presence of proteins and other biological materials do not significantly affect the phase equilibria or the density of the two aqueous phases as the relative amount of proteins and biological material is very small (∼0.2 wt%) compared to the other components.
5. It was assumed that the salt, if present, is distributed equally between top and bottom phases. In reality, the

cations and anions of NaCl are likely to partition to different extent between the phases (Andrews et al., 2005). A detailed model which takes into account partitioning of specific anions and cations was not considered in this work as there is unfortunately currently no experimental data in the literature to support such a model.
6. For the continuous counter-current system, the mass holdup and phase ratio on each stage was assumed to be constant. In practice, one could achieve this using a control scheme made up of inline flow and density meters paired up with control valves.
7. Perfect mixing was assumed, meaning that the composition of the phase outlet streams is assumed to be the same as the phase composition inside the stage. Again, this is a common assumption when considering stage-wise separation models.

2.2. Experimental data

Experimental phase equilibria and protein partitioning data for the case study was obtained from Mistry et al. (1996). Their study examined the partitioning of α-amylase and impurities in a PEG 4000–phosphate ATPS in the presence of NaCl. Their protein partitioning data was used to generate correlations which were used to describe how α-amylase and impurities partition between the top and bottom phases during process simulations. Binary interaction parameters ($\beta_{i,i}$ and $\beta_{i,j}$) required in our model were not considered by Mistry et al. (1996), hence we estimate these in this work but based on their phase equilibria data. These binary interaction parameters were then used in the process model to describe the aqueous two-phase system phase equilibria during process simulations. This study was chosen primarily for the completeness of experimental data which includes both partitioning data as
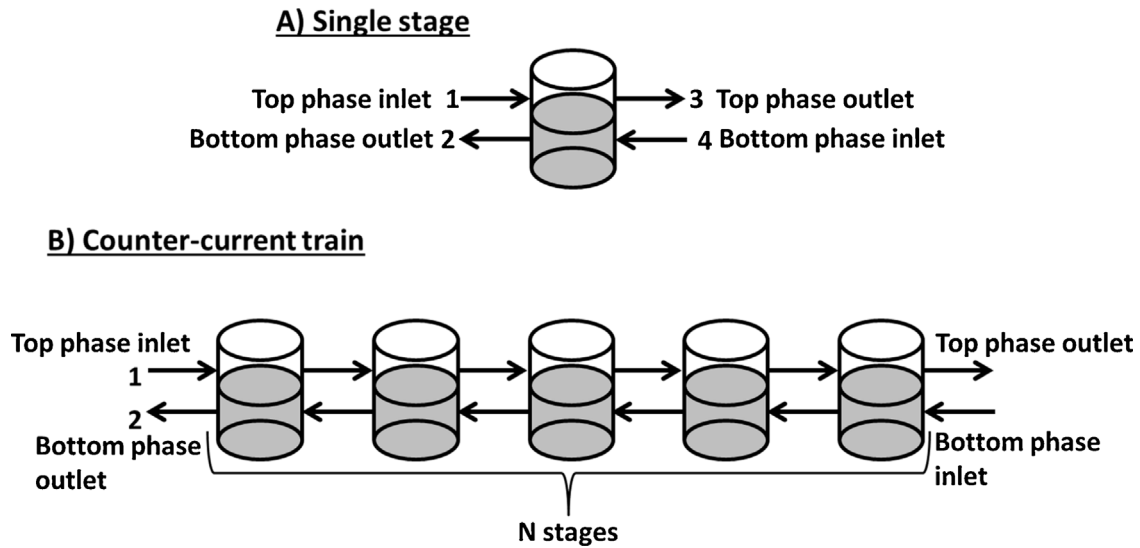
Fig. 2 – (A) Set up of a single ATPS separation stage, (B) a continuous counter-current ATPS separation system.

well as phase diagrams including tie-lines, furthermore, this reduced the need to mix and match experimental data from different literature sources. The required data points were extracted from the experimental figures provided by Mistry et al. (1996) using the digitise tool in OriginPro 8.6 (OriginLab, 2012).

2.3. Process model

The process model described below is a dynamic equilibrium-stage process model which is based on a single stage which can be used to describe both batch and continuous systems.

2.3.1. Mass balances
A simple process model with two inlets and two outlets was used to model both multi-cycle batch and counter-current modes of operation. A single stage as shown in Fig. 2A was used for multi-cycle batch simulations. For continuous counter-current simulations, multiple single stages were connected together as shown in Fig. 2B. This is equivalent to the approach used for distillation and absorption.

The following equations were considered for all components where NC is the number of components: Eq. (1) is an overall mass balance around the stage (stage n) with two inlet streams (streams 1 & 4) and two outlet streams (streams 2 & 3). Eq. (2) is the sum of the mass holdup of all components in the stage in each phase which must add up to the total mass holdup. Eqs. (3) and (4) are a consequence of Assumption 7 i.e. perfect mixing. Eqs. (5)–(7) are definitions of component mass fractions in the system.

For stage n:

$$\frac{dM_{i,overall,n}}{dt} = F_{1,n}x_{i,1,n} - F_{2,n}x_{i,2,n} - F_{3,n}x_{i,3,n} + F_{4,n}x_{i,4,n}$$
$$for\ i = 1...NC \tag{1}$$

$$M_{i,overall,n} = M_{i,top,n} + M_{i,bottom,n} \quad for\ i = 1...NC \tag{2}$$

$$x_{i,3,n} = x_{i,top,n} \quad for\ i = 1...NC \tag{3}$$

$$x_{i,2,n} = x_{i,bottom,n} \quad for\ i = 1...NC \tag{4}$$

$$x_{i,top,n} \times \sum M_{i,top,n} = M_{i,top,n} \quad for\ i = 1...NC \tag{5}$$

$$x_{i,bottom,n} \times \sum M_{i,bottom,n} = M_{i,bottom,n} \quad for\ i = 1...NC \tag{6}$$

$$x_{i,overall,n} \times \sum M_{i,overall,n} = M_{i,overall,n} \quad for\ i = 1...NC \tag{7}$$

2.3.1.1. Initial conditions. As the model is dynamic, holdup in stage n was specified as the initial condition using Eq. (8):

$$M_{i,overall,n} = initial\ value \quad for\ i = 1...NC\ at\ t = 0 \tag{8}$$

2.3.1.2. Additional equations for the continuous counter-current model. Additional equations are needed to link together the stages in the counter-current model shown in Fig. 2B. Stage numbers increase from left to right. NS is the total number of stages:

$$F_{3,n} = F_{1,n+1} \quad for\ n = 1...NS - 1 \tag{9}$$

$$x_{i,3,n} = x_{i,1,n+1} \quad for\ n = 1...NS - 1, \quad i = 1...NC \tag{10}$$

$$F_{4,n} = F_{2,n+1} \quad for\ n = 1...NS - 1 \tag{11}$$

$$x_{i,4,n} = x_{i,2,n+1} \quad for\ n = 1...NS - 1, \quad i = 1...NC \tag{12}$$

In the counter-current model, overall mass hold-up and phase ratio ($\varnothing_n$) in each stage are kept constant as stated by Assumption 6. Eq. (13) defines the phase ratio. Eq. (14) ensures that the phase ratio is constant as it keeps the ratio of $F_{2,n}$ to $F_{3,n}$ equal to the phase ratio. Eq. (15) describes the assumption of constant stage holdup.

$$\varnothing_n \times \sum M_{i,bottom,n} = \sum M_{i,top,n} \quad for\ n = 1...NS \tag{13}$$

$$F_{2,n} \times (\varnothing_n + 1) = F_{1,n} + F_{4,n} \quad for\ n = 1...NS \tag{14}$$

$$F_{1,n} + F_{4,n} - F_{2,n} - F_{3,n} = 0 \quad for\ n = 1...NS \tag{15}$$

2.3.2. Equilibrium descriptions for the case study
2.3.2.1. Partition coefficients and density correlations. The system considered in this case study consists of six components. PEG 4000 (component 1), phosphate (component 2), water (component 3) and NaCl (component 4) establish the ATPS into which the α-amylase (component 5), and the impurities

(component 6), are distributed. The partition coefficients of α-amylase, and the impurities were empirically correlated to the NaCl mass fraction based on the experimental data of Mistry et al. (1996). A polynomial function was used to correlate the α-amylase partition coefficient instead of the sigmoidal Boltzman function used by Mistry et al. (1996), as we found it to fit better when conducting curve fitting:

$$ln(K_{\alpha-amylase,n}) = 0.04874(100 \times x_{NaCl,overall,n})^2 + 0.3043$$
$$\times 100 \times x_{NaCl,overall,n} - 2.731 \quad for \, n = 1...NS \qquad (16)$$

$$ln(K_{impurities,n}) = 0.01412$$
$$\times 100 \times x_{NaCl,overall,n} - 0.01341 \quad for \, n = 1...NS \qquad (17)$$

The equilibrium relationship for proteins is given by Eq. (18) below where $K_{i,n}$ is the partition coefficient for component i in stage n. The equilibrium relationship for NaCl is given by Eq. (19) and is a result of Assumption 5.

$$C_{i,top,n} = K_{i,n}C_{i,bottom,n} \quad for \, i = 5...6, \quad for \, n = 1...NS \qquad (18)$$

$$x_{i,top,n} = x_{i,bottom,n} \quad for \, i = 4, \quad for \, n = 1...NS \qquad (19)$$

The density (in $kg \, m^{-3}$) of each phase was correlated to the mass fraction of PEG 4000, phosphate and NaCl mass fractions as determined by Samatou (2012) who derived the correlation from experimental data:

$$\rho_{q,n} = 1000 + 176 \times x_{PEG4000,q,n} + 888 \times x_{phosphate,q,n} + 808 x_{NaCl,q,n}$$
$$for \, q = top, \, bottom \quad for \, n = 1...NS \qquad (20)$$

2.3.2.2. *Thermodynamic framework*. In this work equations based on osmotic virial expansions were used to calculate the chemical potential (μ_i) of the polymer (component 1), phosphate (component 2) and water (component 3) in terms of molality (m_i), which allows the calculation of the phase equilibria compositions. The equations are based on those reported by Edmond and Ogston (1968) and Zafarani-Moattar and Sadeghi (2001) which have been used to describe PEG-dextran and PEG-salt aqueous two-phase systems, respectively:

$$\mu_1 = \mu_1^0 + RT \left(\ln(m_1) + \beta_{1,1}m_1 + \beta_{1,2}m_2 \right) \qquad (21)$$

$$\mu_2 = \mu_2^0 + RT \left(\ln(m_2) + \beta_{2,2}m_2 + \beta_{1,2}m_1 \right) \qquad (22)$$

$$\mu_3 = \mu_3^0 - RTV_3 \left(m_1 + m_2 + \frac{\beta_{1,1}}{2}m_1^2 + \frac{\beta_{2,2}}{2}m_2^2 + \beta_{1,2}m_1m_2 \right) \qquad (23)$$

At equilibrium, the chemical potential of each component in each phase is the same:

$$\mu_i^{top} = \mu_i^{bottom} \quad for \, i = 1...3 \qquad (24)$$

The μ_i^0 terms in Eqs. (21)–(23) refer to the chemical potential in the standard states. $\beta_{i,i}$ and $\beta_{i,j}$ are binary interaction parameters.

For the system considered in this work, the amount of PEG in the bottom phase was found to be almost negligible. For numerical robustness in the numerical solution, therefore, its mass fraction was assumed to be constant at a very small value in this phase ($x_{1,bottom} = x_{PEG,bottom} = 0.0001$). This assumption will not have any impact on the results, but is required to ensure stability of the mathematical solution.

2.4. Simulation methodology

All the equations were solved simultaneously as one equation set using gPROMS (Process Systems Enterprise, 2017). Although the model may appear simple, the presence of the equilibrium conditions imposed by Eq. (24) means that initialisation is difficult as good initial estimates are needed, however, this was tackled using the initialisation protocol of gPROMS.

A key focus of this work is the study of how upstream variability may have an impact on the performance of the separation section, in this case, the aqueous two-phase system (ATPS). We describe this variability by an average value and a standard deviation. The feed compositions of the input streams were therefore varied using the normal probability distribution assignment in gPROMS which picks a random value of a parameter or variable given an average value and the corresponding standard deviation.

2.5. Parameter estimation of interaction parameters

Although the description of the PEG 4000–phosphate phase equilibria data was based on the work by Mistry et al. (1996), their empirical correlations were not considered because firstly they required too many fitted parameters which reduces the statistical confidence in each parameter, and secondly the use of thermodynamics to describe phase equilibria allows for a model based on greater fundamental principles, hence Eqs. (21)–(23) were used instead. The interaction parameters, ($\beta_{i,i}$ and $\beta_{i,j}$), therefore needed to be estimated using the experimental tie-line data from Mistry et al. (1996). The estimation of the interaction parameters, $\beta_{i,i}$ and $\beta_{i,j}$, was conducted using the parameter estimation entity in gPROMS. This entity estimates parameters based on Maximum Likelihood which takes into account experimental variation. Since an experimental variation was not provided by Mistry et al. (1996), a standard deviation of 2 wt% was assumed in order to illustrate our methodology, which is conservative for composition mass fractions. The NLPSQP (nonlinear programming sequential quadratic programming) solver in gPROMS was used for the parameter estimation.

3. Results and discussion

In this work, we present an approach based on a dynamic stage-by-stage equilibrium model that can be used to simulate aqueous two-phase extraction (ATPE) processes under a variety of configurations and operating policies. The approach permits a fast, yet systematic, investigation of both process design and process operation for the separation of biomolecules using aqueous two-phase extraction. In the following, we will demonstrate this approach using a case study involving the separation of enzyme α-amylase from impurities in a PEG 4000–phosphate aqueous two-phase system (ATPS) in the presence of NaCl.

Table 1 – Estimated interaction parameters ($\beta_{i,j}$) for Eqs. (21)–(23) in a PEG 4000 (component 1)–phosphate (component 2) aqueous two-phase system.

$\beta_{i,j}$ (kg mol^{-3})	PEG 4000		Phosphate	
	Value	Standard deviation	Value	Standard deviation
PEG 4000	−10.5	5.8	6.1	1.5
Phosphate	6.1	1.5	−1.1	0.1

In the following, we will first examine the quality of the phase equilibria descriptions determined using the estimated interaction parameters for Eqs. (21)–(23). This is an important first step of any model development as it is not possible to model ATPS processes, or any separation process for that matter, without accurate representation of the phase equilibria. Next, we consider a batch extraction process operated over multiple cycles to show the power of dynamic modelling for even a simple process, and how simulations can be used to predict the behaviour of the process. Finally, we investigate the impact of upstream variability on a continuous counter-current extraction process. This is especially important given the demand for quality by design in manufacturing processes which requires the specification of a robust design space.

3.1.   Estimation of $\beta_{i,j}$ parameters

The top and bottom phase compositions of PEG 4000 (component 1) and phosphate (component 2) in their respective phases at different NaCl concentrations were obtained from the experimental tie-lines reported by Mistry et al. (1996). The feed composition was taken to be the mid-point of the tie-line of each respective tie-line since this information was not provided. The parameter estimation entity in gPROMS (Process Systems Enterprise, 2017) is capable of determining the uncertainty in the fitted parameters (standard deviation) given information regarding the experimental uncertainty in the data used for the fitting. This accumulated uncertainty is important to consider (as a small uncertainty may in some cases still lead to a large uncertainty in the fitted parameter values) but is unfortunately often ignored. Since the actual experimental uncertainty was unknown, a conservative standard deviation of 2 wt% in equilibrium phase compositions was assumed as discussed above.

The resulting estimated values of the interaction parameters are reported in Table 1. The PEG 4000–PEG 4000 interaction parameter ($\beta_{1,1}$) has a standard deviation (5.8) which is in the same order of magnitude as the parameter value (−10.5), suggesting that there is insufficient experimental data, or that the assumed uncertainty in the data is too high, in order to estimate this parameter accurately. The PEG 4000–phosphate and phosphate–phosphate interaction parameters (($\beta_{1,2}$) and ($\beta_{2,2}$) respectively), have much lower standard deviations, which means that the uncertainty associated with these parameters is lower.

Parity plots were used to compare model predictions of tie-line compositions (y-axis) to experimental tie-line compositions (x-axis) for the different NaCl concentrations (Fig. 3). A perfect model fit would have all points lie on the line y = x. Parity plots A and B in Fig. 3 for 0 wt% NaCl show a poor model fit. This is likely due to the assumptions made in the development of our model since our model does not take into account electrolyte interactions which we know are present,

but for which we have no experimental data which can be used for parameter estimation. In our model, NaCl does not explicitly interact with PEG 4000 and phosphate, and the presence of NaCl only reduces the overall mass fraction of water, which in turn increases the molality of PEG 4000 and phosphate. Nevertheless, the changes in PEG 4000 and phosphate molality due to NaCl presence are still not significant enough to describe a PEG 4000–phosphate aqueous two-phase system from 0 wt% to 10 wt% NaCl. However, for systems containing NaCl concentrations above 2 wt%, the parity plots show that the phase equilibria predictions are sufficiently accurate for process simulations as the experimental tie-lines reported for these systems by Mistry et al. (1996) are very similar. If a good model fit is required at 0 wt% NaCl then parameter estimation could be conducted using tie-line data of only the 0 wt% NaCl phase diagram, this however is undesirable since it would result in two sets of parameters.

The PEG 4000 mass fraction in the bottom phase is usually very small, therefore a constant mass fraction of 0.0001 was assumed in the simulations to increase the numerical robustness as explained earlier, hence no parity plot is shown for this concentration. The presence of NaCl can be taken into account by extending the chemical potential equations (Eqs. (21)–(23)) to a 4 component system; however, this would require more interaction parameters to be estimated, and sufficient experimental data would need to be available to ensure statistically significant parameters values to be found. As for all parameter estimations, there needs to be a balance between the number of parameters that are to be estimated and the amount of useful experimental data available for parameter estimation. This is because, as the number of parameters is increased, the ability to estimate parameters with low uncertainty decreases. The uncertainty in the estimated parameter values can be reduced in two ways:

1. Reducing the uncertainty in experimental measurement values, in this case 2 wt% error was assumed.
2. Increasing the number of experimental data points, e.g. using Design of Experiments, or model-based experimental design, to determine which experiments should be conducted next so that the most information can be obtained using the fewest possible resources.

Often, reducing the uncertainty in measurements is difficult as it may require development of new experimental techniques which could be costly. Model based experimental design is useful if a model is known to be a good representation of experimental data, however, often one still needs an initial set of experimental data to estimate initial parameters (Dechambre et al., 2014; Tulsyan et al., 2012).

3.2.   Multi-cycle batch extraction simulations

The process model developed in this work can be used to describe the operation of a batch extractive process for an ATPS. The process is simple to operate, and if the purity required is not obtained directly in the first batch, the process can be repeated over another cycle by removing the solvent (bottom) phase, reloading the tank with pure solvent, and repeating the separation as shown in Fig. 4. The separation achieved will thus depend not only on the salt concentration and the phase ratio, but also on the number of cycles considered. Note that to increase purity using this method of

A) PEG top

B) Phosphate top
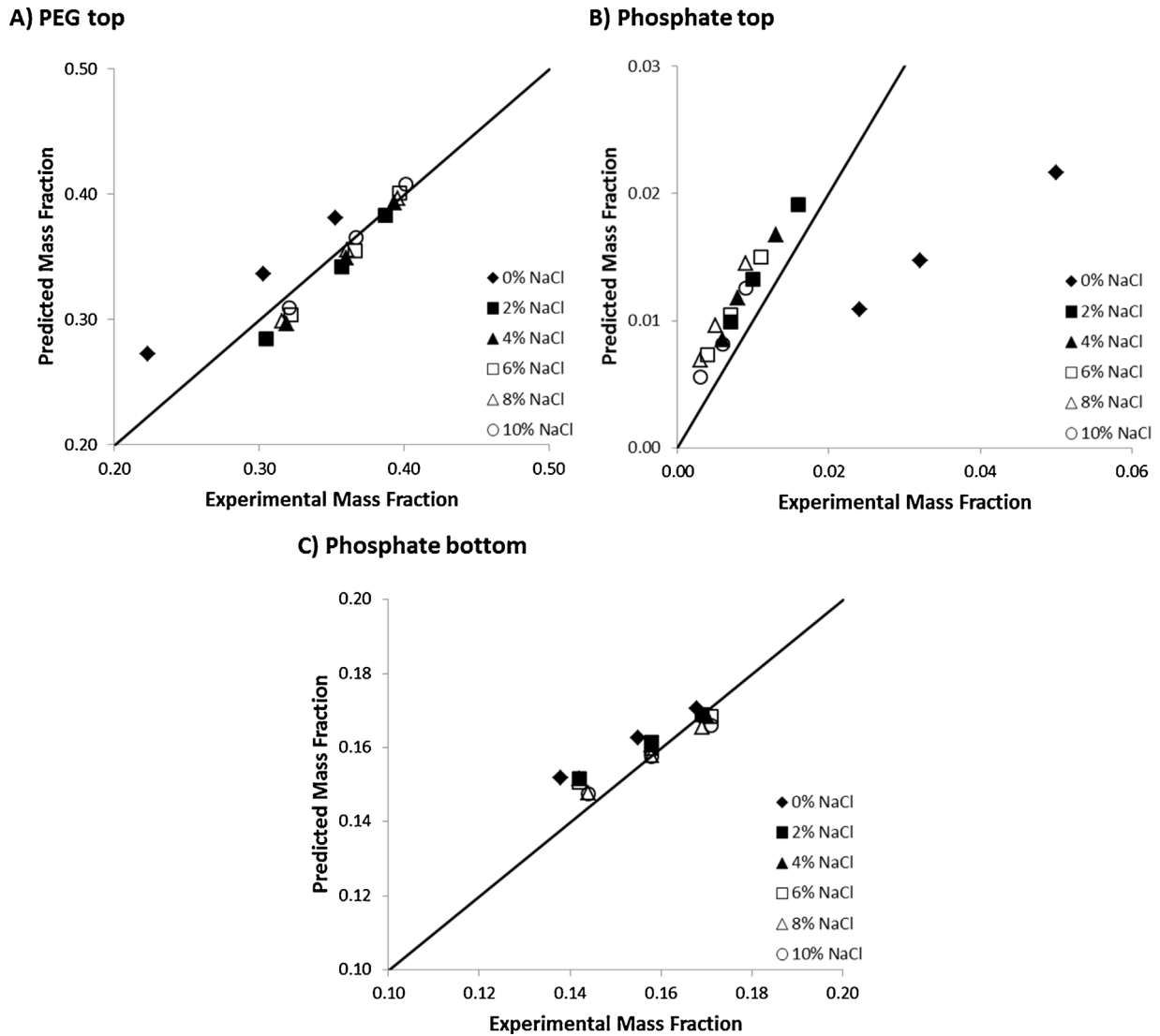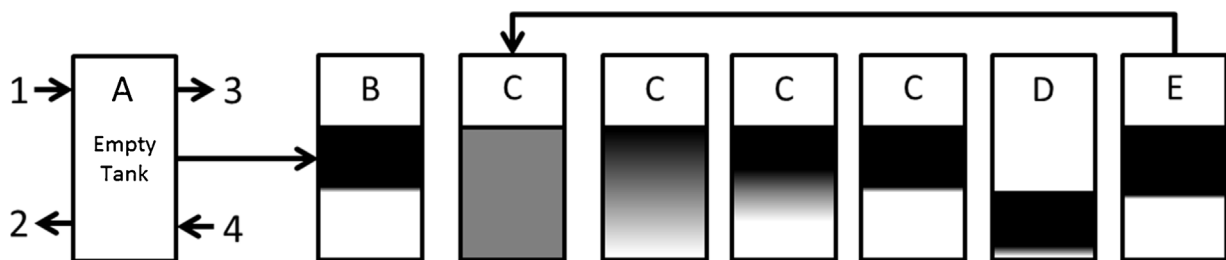

C) Phosphate bottom

Fig. 3 – Parity plots for a PEG 4000–phosphate aqueous two-phase system from 0 wt% to 10 wt% NaCl. Experimental data were obtained from Mistry et al. (1996). (A) PEG top phase mass fraction. (B) Phosphate top phase mass fraction. (C) Phosphate bottom phase mass fraction.

A.   Initially the tank is empty.
B.   Streams 1 (containing target protein) & 4 are turned on until the mass in the tank is greater than 300 kg. (Stream 1 contains the protein).
C.   Allow 10 minutes for mixing and 15 minutes for settling. (Mixing and settling is not modelled).
D.   Drain the bottom phase (containing target protein) via stream 2 (1 kg s⁻¹) until the mass in the bottom phase is less than 5 kg.
E.   Fill with fresh phosphate rich bottom phase via stream 4 until the mass in the tank is greater than 300 kg. Go to step C.
Repeat steps C to E for multiple extraction cycles.

Fig. 4 – Schematic of operating protocol for multi-cycle batch extraction for case study. Operating multiple extraction cycles is useful for increasing process purities, however, yields are decreased due to loss of product when replenishing the removed phase.

Table 2 – Operating conditions considered for multi-cycle batch extraction of α-amylase (component 5) with impurities (component 6) in a PEG 4000 (component 1)–phosphate (component 2) aqueous two-phase system.						
Stream #	Operating flow rate (kg s⁻¹)	α-amylase concentration (kg m⁻³)	Impurity concentration (kg m⁻³)	PEG (wt%)	Phosphate (wt%)	NaCl (wt%)
1	1.00	1.00	1.00	27.38	1.77	6–10
4	1–4.00	N/A	N/A	0.01	14.46	6–10

Table 3 – Operating conditions considered for continuous counter-current extraction of α-amylase (component 5) with impurities (component 6) in a PEG 4000 (component 1)–phosphate (component 2) aqueous two-phase system (phase ratio ∼ 1).						
Stream #	Operating flow rate (kg s⁻¹)	α-amylase concentration (kg m⁻³)	Impurity concentration (kg m⁻³)	PEG (wt%)	Phosphate (wt%)	NaCl (wt%)
1 in stage 1	0.00347	0 or 0.325	0 or 0.325	27.38	1.77	6–10
4 in last stage	0.00347	0 or 0.325	0 or 0.325	0.01	14.46	6–10

multi-cycle batch extraction will result in a reduced product yield.

The operation of a batch operated ATPS over a number of extraction cycles was considered first, as most biopharmaceutical operations are currently operated either batch-wise or semi-batchwise. The streams profiles are shown in Table 2 and are based on Fig. 2A. Streams 1 and 4 feed the PEG rich top phase and phosphate rich bottom phase, respectively. The influence of the phase ratio (mass of top phase to mass of bottom phase) on yield and purity was investigated by varying the mass flow rate of stream 4 during initial loading. A detailed schematic of the operating protocol used can be found in Fig. 4. The responses in Figs. 5 and 6 at 30 min intervals correspond to the extraction cycles outlined in the operating protocol. The flat sections in Figs. 5 and 6 consisting of ∼7 data points each correspond to the time associated with mixing (10 min) and settling (15 min).

3.2.1. Extraction cycles

The purity, i.e. the ratio of α-amylase concentration to total concentration of α-amylase and impurities, can be improved by repeating the extraction process over a number of cycles. Increasing the number of extraction cycles is akin to increasing the number of stages in a continuous counter-current process. The advantage of a multi-cycle batch setup is that this operation is simple to execute as the product is just recycled back to the tank and the process runs again for each cycle.

As expected, increasing the number of extraction cycles results in a higher purity of protein (α-amylase) in the product (top) phase, however, this comes at the cost of a reduced yield (see Fig. 5). The yield is reduced because for each new extraction cycle, more α-amylase is being lost to the fresh bottom phase (contains no α-amylase or impurities) as a new equilibrium is established. In addition, one must also consider whether the reduction in concentration as a result of increasing the number of extraction cycles is worthwhile since, as shown in Fig. 6, each cycle results in more material being lost, therefore the maximum achievable concentration is reduced.

3.2.2. Amount of NaCl

Fig. 5 shows that increasing the NaCl concentration from 6 wt% to 10 wt% will cause both the purity and the yield to increase. This is because the partition coefficient of α-amylase is increased almost 90-fold as the salt concentration is increased, whilst the partition coefficient of the impurities remains relatively constant. This can be explained by

the differences in the correlations for the partition coefficient described by Eqs. (16)–(17). The addition of salts often results in the partition coefficient of proteins changing, however, the magnitude and direction of this change differs between proteins (Tubio et al., 2007; Gunduz and Korkmaz, 2000). This effect is most noticeable in plot B in Fig. 6 where the concentration of impurities in the top phase remains almost identical at both 6 wt% and 7 wt% NaCl. Operating using 10 wt% NaCl would see a purity and yield of 0.86 and 0.98 after three extraction cycles, respectively. At NaCl concentrations less than 5 wt%, the α-amylase partition coefficient is less than 1, meaning that the operating protocol could be adapted to replace the top phase instead of the bottom phase, thus allowing for the product to be loaded into the bottom phase. This could be useful for situations where a high salt concentration feed is required for the next purification step such as in hydrophobic interaction chromatography.

3.2.3. Phase ratio

Fig. 5 also shows how the phase ratio can be manipulated to alter purity and yield. A smaller phase ratio (plots C & D) results in higher purity because, relative to α-amylase, more impurities partition into the bottom phase. Unfortunately, the amount of α-amylase in the bottom phase is also increased when the phase ratio is decreased, hence resulting in a lower yield.

3.3. Continuous counter-current simulations

Although batch operation is currently the preferred mode of operation for biopharmaceuticals, there is a drive towards continuous operation where possible, due to the increased efficiency associated with these processes. To consider continuous operation of the ATPS system, a base case study of a perfusion bioreactor setup was considered. Perfusion bioreactors are well suited to a continuous counter-current setup because they can be set up so that there is a continuous flow of cell culture material containing the product of interest to subsequent downstream separations.

In the case study, a perfusion bioreactor of 300 l was assumed with a perfusion rate of 300 l per day (i.e. 1 reactor volume). Pollock et al. (2013) state that product titre in a fed-batch setup can range from 2 to 10 g/l. In addition, they state that the titre in a perfusion setup can range from 20% to 45% of the fed-batch setup. Assuming a fed batch titre of 2 g/l, a perfusion titre of 0.65 mg ml⁻¹ was used in the follow-
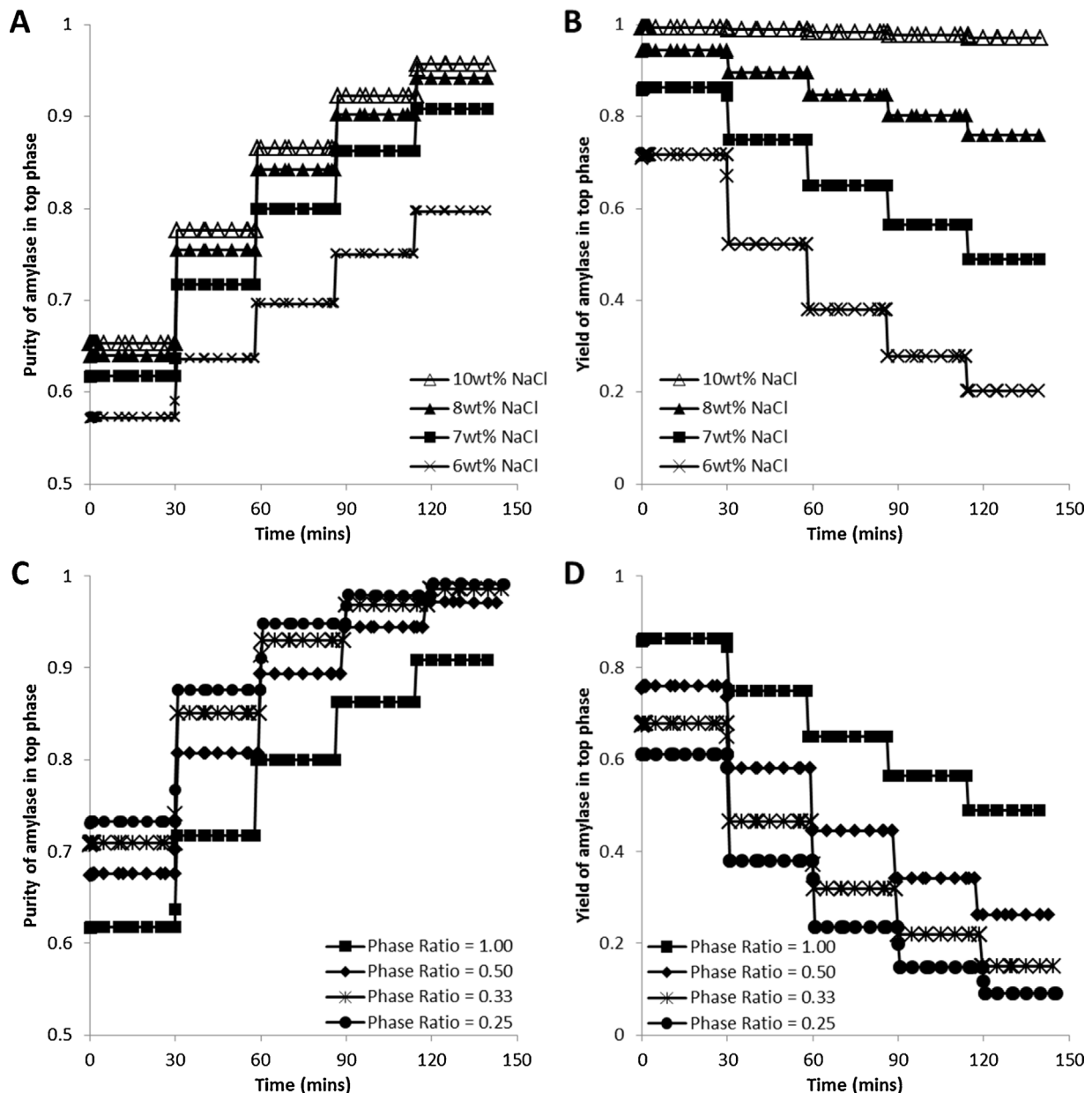
Fig. 5 – Simulated protein (α-amylase) yield and purity in the top phase of a PEG 4000–phosphate aqueous two-phase system multi-cycle batch extraction process. The steps of 30 min duration correspond to time associated with mixing, settling and draining as shown in points C–E in Fig. 4. The changes in step height correspond to refilling the tank with fresh bottom phase as shown in point E in Fig. 4. (A & B) Influence of NaCl concentration (phase ratio ∼ 1). (C & D) Influence of phase ratio (7 wt% NaCl).

ing for both product and impurities. The flow rate of the feed is based on a perfusion rate of 300 l per day assuming a density of ∼1000 kg m^{-3}. The feed composition of protein (α-amylase) and impurities was set to half of the perfusion titre, i.e. a 1× dilution factor, because in reality one would have to dilute the perfusion culture feed with the polymers, salt and water. Specific details of stream compositions can be found in Table 3. The initial compositions in each stage are shown in Table 4.

3.3.1. Feed location
So far, it has been assumed that the proteins (α-amylase and impurities) are introduced to the system in the top PEG 4000 rich phase and that the phosphate rich bottom phase is used as the solvent to extract impurities. The model can be used to explore how changing the feed location of the proteins from the top (PEG 4000) to the bottom (phosphate) phase may influ-

Table 4 – Initial composition of each stage for continuous counter-current extraction of α-amylase in a PEG 4000 (component 1)–phosphate (component 2) aqueous two-phase system (phase ratio ∼ 1).

Variable	Symbol	Value
Mass hold up (kg)	–	2 or 10
Composition of PEG 4000	$w_{1,overall,n}$ (wt%)	13.7
Composition of phosphate	$w_{2,overall,n}$ (wt%)	8.2
Composition of NaCl	$w_{4,overall,n}$ (wt%)	6–10

ence the accumulated protein purity. Fig. 7 shows this scenario for a 3 stage system where the feed location of protein is changed from stage 1 (top) to stage 3 (bottom). As can be seen, the switch from the top to the bottom phase results in a reduction in purity from ∼0.75 to ∼0.57 for the protein (α-amylase). This is because when α-amylase is fed in the top phase (stage
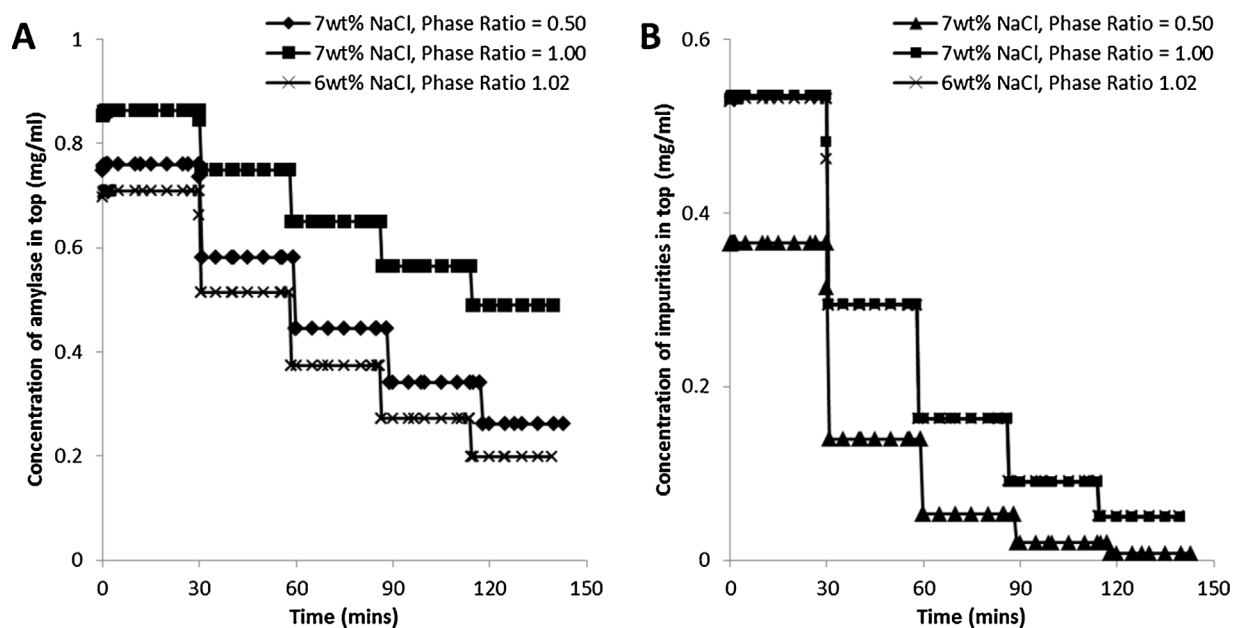
Fig. 6 – Concentration of protein (α-amylase) (A) and impurities (B) changes as a result of NaCl, phase ratio and extraction cycles in a PEG 4000–phosphate aqueous two-phase system multi-cycle batch extraction process. The steps of 30 min duration correspond to time associated with mixing, settling and draining as shown in points C–E in Fig. 4. The changes in step height correspond to refilling the tank with fresh bottom phase as shown in point E in Fig. 4.

1), there is more efficient utilisation of each extraction stage as a result of the system maintaining a larger concentration difference between the phases across all stages due to there being a α-amylase partition coefficient value greater than 1. This can be clearly seen in plot C in Fig. 7 where the concentration difference of α-amylase between the phases remains higher than 0.20 mg ml^{-1} for all three stages when fed via the top phase. Plot D in Fig. 7 shows how the concentration difference drops dramatically from stage 3 to 1, therefore resulting in most of the purification of α-amylase happening in stage 3 for the bottom phase fed scenario, and hence a less efficient utilisation of the 3 stages. These findings will change depending on the partitioning characteristics of the components. If, for example, the desired product had a partition coefficient value smaller than 1, then it would make more sense to feed via the bottom phase.

3.3.2.   Influence of NaCl variability

The partitioning of α-amylase and impurities between the two phases is also influenced by the amount of NaCl in the aqueous two-phase system, as well as by the scale of the operation. To understand the importance of NaCl we investigate the sensitivity of process performance due to poor control of NaCl in the process feeds of the first and final stage. NaCl is present throughout the whole separation system; this can only be achieved if NaCl is fed via streams in both first and final stages. Therefore it was important to consider poor control of NaCl in both these feed streams. As outlined below, the variability was considered by randomly assigning the NaCl wt% value based on a normal probability distribution with a mean of 7 wt% and a standard deviation of 2 wt%. A random value is chosen every 60 s after ~8.5 h of continuous operation.

NaCl concentration in stream 1 of stage 1 is normally distributed:

$$x_{NaCl,1,1} \sim N\left(7wt\%, 2wt\%\right)$$

NaCl concentration in stream 4 of stage NS is normally distributed:

$$x_{NaCl,4,NS} \sim N\left(7wt\%, 2wt\%\right)$$

Variations were started after ~8.5 h because this is when the simulated concentration of α-amylase in the top phase of the final stage was at steady-state. Fig. 8A shows how when the variability is introduced, the concentration of α-amylase fluctuates as a result. The difference between the maximum and minimum concentrations (i.e. the range) of α-amylase after start of variations is 0.11 mg ml^{-1} which is 38% of the mean α-amylase concentration value (0.28 mg ml^{-1}). Such product concentration variations due to inherent process variability may be very important to control because they could have serious implications on subsequent separation stages where the tolerance of the feed material being processed is quite stringent. The model has shown the impact of this particular variation and can also be used to investigate others (not shown).

3.3.3.   Influence of stage size on variability

One way to control variability is to have a system which is inherently less susceptible to disturbances; this can be achieved by increasing the size of the system. Plots A and B in Fig. 8 show how simply increasing the size of the system, i.e. changing the total amount of holdup in each stage from 2 kg to 10 kg, results in a dampening effect when the NaCl wt% of the feed streams starts to randomly vary based on the same mean value and standard deviation as before. This is because the flow rates going into the aqueous two-phase system are kept the same while the system itself is larger and therefore less susceptible to disturbances. For the 10 kg stage holdup system, the difference between the maximum and minimum α-amylase concentrations after start of variations is 0.04 mg ml^{-1} which is 14.8% of the mean α-amylase concentration value (0.28 mg ml^{-1}). This is less than 40% of the range observed in the 2 kg holdup system. In addition, the resulting relative standard deviation for the downstream α-
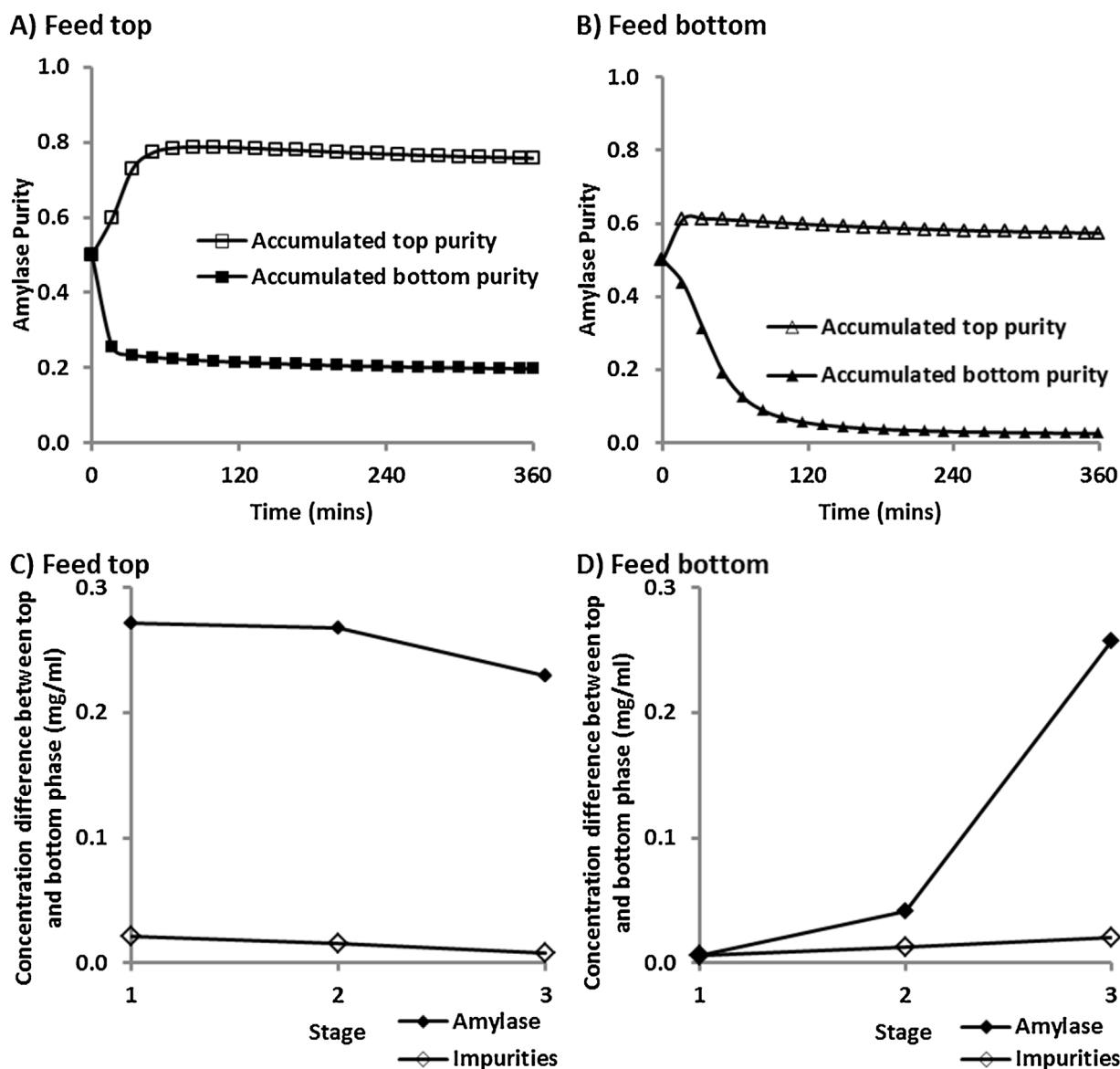
Fig. 7 – Influence of feed location on process design and purification performance of a 3 stage counter-current operation of a PEG 4000–phosphate ATPS (7 wt% NaCl, phase ratio ∼1). Plots A & C: feeding protein in stage 1 stream 1 (top phase). Plots B & D feeding protein in stage 3 stream 4 (bottom phase). Plots C & D: are concentration differences between top and bottom phase in each stage at 360 min.

amylase concentration in the top phase of the final stage of the ATPE, for both 10 kg and 2 kg stage holdups, is 7.08% and 2.50%, respectively. The model has here been used to show one example of how a modelling approach can be used to investigate process behaviour following uncertainties for different designs. The severity of the impact of these uncertainties will entirely depend on the requirements and robustness of subsequent downstream separation processes.

It should be noted that one disadvantage of increasing the holdup mass of each stage is that the length of time taken to reach steady-state of the yield is increased (see Fig. 8C); this may, however, be insignificant if one is running a 60 day perfusion culture.

3.3.4. Influence of drifting product titre and number of stages

The model can also be used to investigate the impact of a drifting titre over the course of a 65 day perfusion. Product titre is likely to change due to the inherent variability associated with producing products using living organisms. Fig. 9 shows a case

where the product and impurity titre were kept constant for the first 5 days of operation and was then allowed to decay as shown in Fig. 9. The new decayed concentration of α-amylase is 0.3% less than the α-amylase concentration in the previous 24 h while the new non-decaying impurity concentration is 0.3% higher than the impurity concentration in the previous 24 h i.e.

$$C_{1,new,\alpha\text{-}amylase} = 0.997 \times C_{1,old,alpha\text{-}amylase}$$

$$C_{1,new,Impurities} = 1.003 \times C_{1,old,Impurities}$$

where the old concentrations are randomly chosen from a normal distribution of the concentration in the past 24 h and with a standard deviation of 0.001:

$$C_{1,old,alpha\text{-}amylase} \sim N \,(Concentration\ of\ \alpha\text{-}amylase\ in\ previous$$
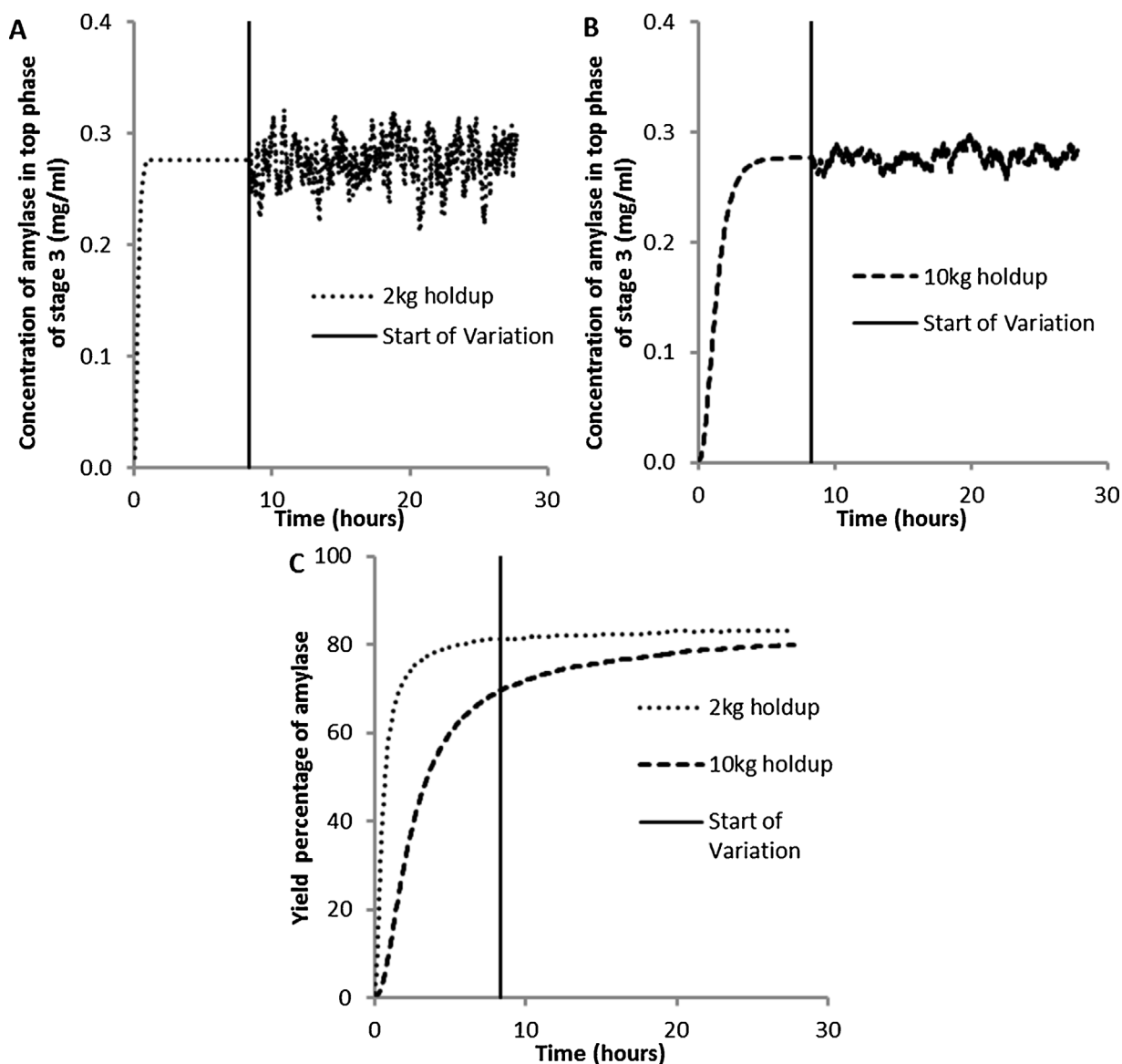
$$24\,h,\ 0.001)$$

Fig. 8 – (A & B) Impact of NaCl (mean 7 wt%, standard deviation 2 wt%) variability on α-amylase concentration in the top phase of the final stage in a 3 stage continuous counter-current extraction process with 2 kg and 10 kg stage holdup. Variation of NaCl is implemented once start-up is completed (i.e. when there is a steady-state concentration of α-amylase). (C) Total yield percentage of α-amylase with 2 kg and 10 kg stage holdup.

$$C_{1,old,Impurities} \sim N \, (Concentration \, of \, impurities \, in \, previous$$

$$24 \, h, \, 0.001)$$

Plot B in Fig. 9 shows how the purity of α-amylase out of each stage decreases as the titre drifts. Although the product purity in the feed drops from 50% to ∼42% over the simulated 65 days, the absolute drop in α-amylase purity (purity before titre drift minus purity at end of simulation) is ∼6.5%. In this simulation, 7 wt% NaCl was assumed which results in an α-amylase partition coefficient of ∼8.5. Fig. 10 shows how increasing the number of counter-current stages from 3 to 24 influences process purity. For simulations conducted using 24 stages there is a high purity at the start which drops sharply, this is due to fact that during model initialisation there is a small but non-zero (1×10^{-5} kg) amount of α-amylase and impurities in stage 24. As the material from stage 1 reach stage 24, the purity rapidly drops to the true purity. If the same simulation is run but with 12 counter-current stages instead of 3

stages, an absolute purity drop of ∼4.7% is observed. Fig. 10B shows that increasing the number of stages results in a smaller drop in purity; however, it seems that the drop in purity is not linear with number of stages suggesting that after a certain number of stages are added, the benefit gained in terms of purity drop is negligible. In addition to reducing the drop in purity, increasing the number of stages 3–24 increases the total of α-amylase purity from 67% to 83% respectively; this is similar to increasing the number of cycles in the multi-cycle batch setup. This is as expected for stage-wise separation processes.

The results presented in this work have shown how even a relatively simple mathematical model can be used to better understand robustness of operation under dynamic conditions when disturbances or other changes may influence the process, which is often difficult or impossible to gauge when using steady-state process models. If more accurate models were available, then these could be used directly for process design and financial analysis in order to find the optimal design and the most appropriate mode of operation.
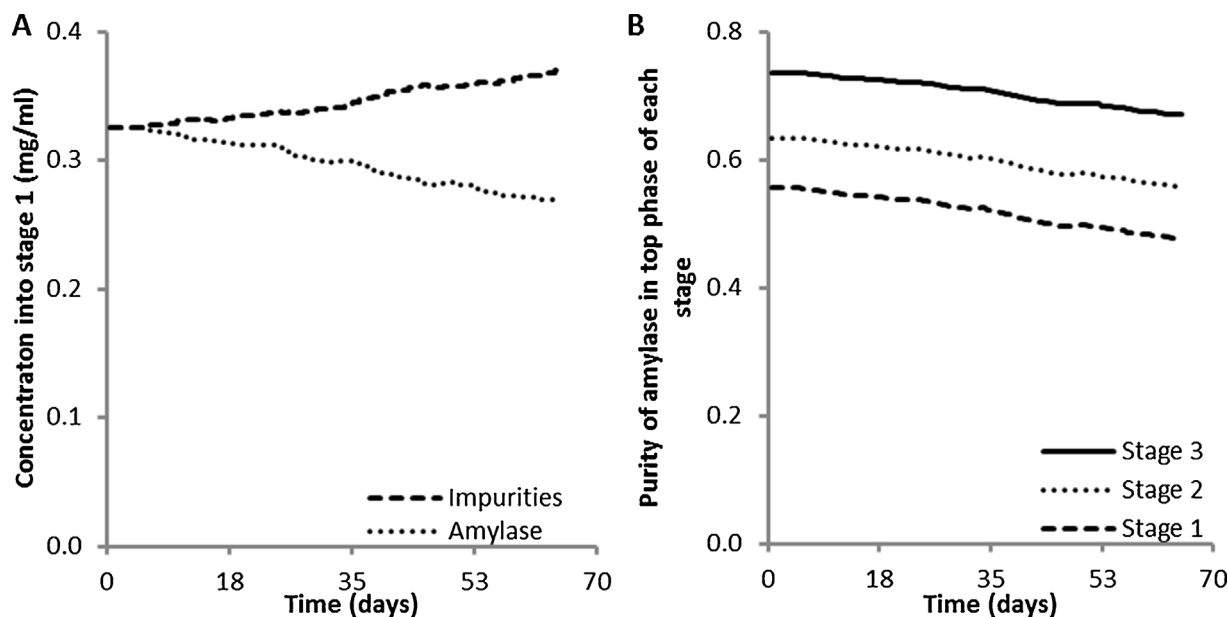
Fig. 9 – Impact of drifting titre (increasing impurities & decreasing product) on purity in a 3 stage continuous counter-current extraction process. (NaCl kept constant at 7 wt%.). (A) Titre of α-amylase and impurities into stage 1. (B) in-line purity of α-amylase in the top phase of each stage of the counter-current train.
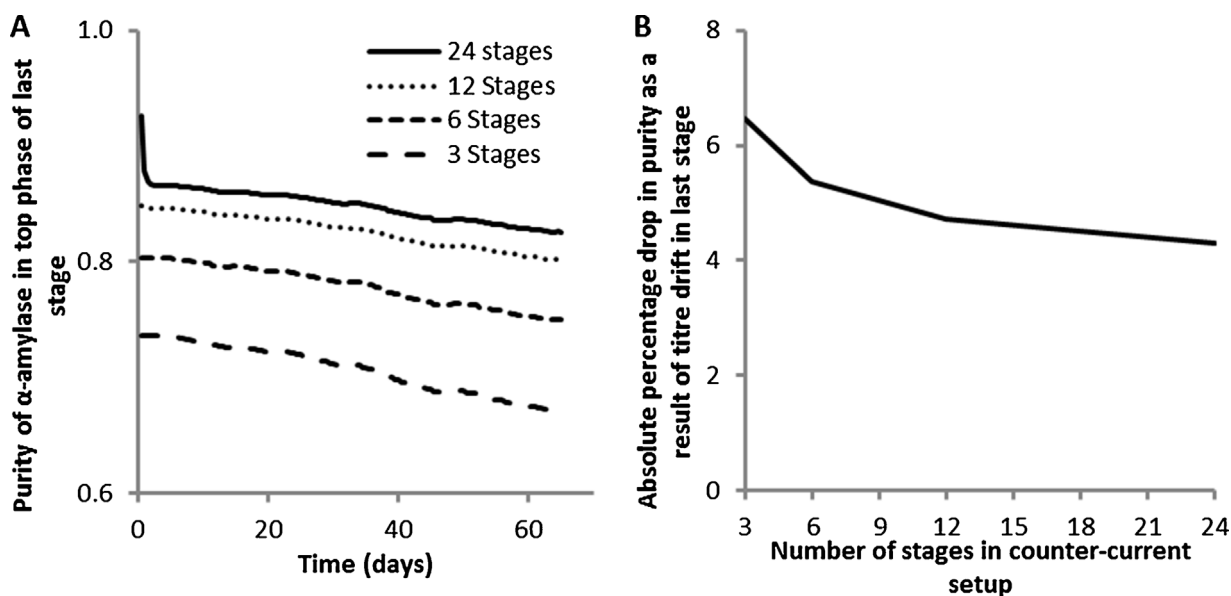

Fig. 10 – Impact of process design on product purity in the presence of drifting titre. (A) Influence of number of stages on in-line purity of α-amylase in final stages, and (B) Influence of number of stages on absolute drop in purity.

3.4. Advantages, limitations and challenges of this modelling approach

The main advantages of the approach presented in this work for the modelling and simulation of aqueous two-phase systems are:

1. Flexibility to use one model to investigate different modes of operation such as multi-cycle batch and continuous counter-current modes of operation, as well as the flexibility to adapt the model to different experimental systems using appropriate parameter estimation and description of component partitioning.
2. The ability to conduct dynamic simulations which are extremely important in understanding impact of bioprocess variability.

3. The inclusion of thermodynamic equations to describe phase equilibria which is something current literature has not considered for aqueous two-phase system process simulations.

Important limitations to the modelling approach presented include the need to validate model simulations with experimental data, for example stage efficiency which is unlikely to be 100%. In addition, the approach presented in this work considered only two components, α-amylase and impurities, as all other components generated during upstream fermentation/cell culture are lumped together as impurities. These components could be considered individually. To be able to model these types of multi-component systems will require a careful balance of model detail and experimental effort as the experimental effort would be phenomenal. One solution to

this is to use high-throughput analytical techniques to quantify only the major impurity types.

3.5. *General experiments required for future modelling of aqueous two-phase systems*

In this work experimental data produced by Mistry et al. (1996) was used for model training. To model different types of products and of aqueous two-phase systems requires the generation of further experimental data. The two types of experimental data required are:

1) Phase equilibria data in the form of phase diagrams for the specific aqueous two-phase systems being used e.g. PEG–phosphate, PEG–citrate etc.
2) Product and impurity partitioning data within the specific aqueous two-phase systems being considered e.g. α-amylase or monoclonal antibody partitioning data in a PEG-phosphate aqueous two-phase system

Experimental phase diagrams are required to estimate appropriate parameters used in process models to describe how aqueous two-phase system components partition between the two established phases e.g. the amount of PEG in the top phase and phosphate in the bottom phase. The amount of experimentation required can be reduced for new products by ensuring that experimentally determined phase diagrams are of a high quality and well documented so that they can be re-used for many different products. To reduce experimentation further, phase diagrams can also be obtained from literature sources, however, it is advised that such phase diagrams are validated to ensure they are representative of the systems being considered.

Product partitioning data in specific aqueous two-phase systems need to be determined experimentally for each new product. This is because currently it is difficult to predict how a specific product will partition a priori. The resultant experimental partitioning data can then be used to determine empirical correlations that can be used in process models such as presented in this work.

4. Conclusions

The main aim of this work was to present a dynamic equilibrium stage process model, and a methodology for prediction of key process parameters from limited experiments, capable of describing aqueous two-phase extraction (ATPE) separations under both multi-cycle batch and continuous counter-current modes of operation. The model can be used to predict the separation performance of the process, as well as for the investigation of suitable design and operating conditions.

The capabilities of the methodology was demonstrating using a case study of a PEG 4000–phosphate–NaCl aqueous two-phase extraction (ATPE) process for the purification of α-amylase using both multi-cycle batch or continuous counter-current extraction modes. Thermodynamic interaction parameters were estimated from experimental phase equilibria data from literature, and were found to be sufficiently accurate for phase equilibria predictions for aqueous two-phase systems (ATPSs) containing more than 2 wt% NaCl.

In this work, we have demonstrated how a relatively simple dynamic process model can be used to better understand the behaviour of the aqueous two-phase extraction system, and to predict process behaviour of downstream processing as a result of upstream product variability. The development of the model also involved estimation of model parameters from a limited number of experiments, and an analysis of the impact of experimental uncertainty on the accuracy of the parameters obtained.

References

Andrews, B.A., Schmidt, A.S., Asenjo, J.A., 2005. Correlation for the partition behavior of proteins in aqueous two-phase systems: effect of surface hydrophobicity and charge. Biotechnol. Bioeng. 90, 380–390.

Asenjo, J.A., Andrews, B.A., 2011. Aqueous two-phase systems for protein separation: a perspective. J. Chromatogr. A 1218, 8826–8835.

Biegler, L.T., Grossmann, I.E., 2004. Retrospective on optimization. Comput. Chem. Eng. 28, 1169–1192.

Cabezas, H., 1996. Theory of phase formation in aqueous two-phase systems. J. Chromatogr. B: Biomed. Appl. 680, 3–30.

Chen, C.C., Mathias, P.M., 2002. Applied thermodynamics for process modeling. AIChE J. 48, 194–200.

Dechambre, D., Wolff, L., Pauls, C., Bardow, A., 2014. Optimal experimental design for the characterization of liquid–liquid equilibria. Ind. Eng. Chem. Res. 53, 19620–19627.

Don, W.G., Robert, H.P., 2008. Simulation of distillation processes. In: Perry's Chemical Engineers' Handbook, 8th ed. McGraw Hill Professional, Access Engineering.

Ecker, D.M., Jones, S.D., Levine, H.L., 2015. The therapeutic monoclonal antibody market. Mabs 7, 9–14.

Edmond, E., Ogston, A., 1968. An approach to the study of phase separation in ternary aqueous systems. Biochem. J. 109, 569–576.

Gunduz, U., Korkmaz, K., 2000. Bovine serum albumin partitioning in an aqueous two-phase system: effect of pH and sodium chloride concentration. J. Chromatogr. B 743, 255–258.

Hendriks, E., Kontogeorgis, G.M., Dohrn, R., De Hemptinne, J.C., Economou, I.G., Zilnik, L.F., Vesovic, V., 2010. Industrial requirements for thermodynamics and transport properties. Ind. Eng. Chem. Res. 49, 11131–11141.

Huenupi, E., Gomez, A., Andrews, B.A., Asenjo, J.A., 1999. Optimization and design considerations of two-phase continuous protein separation. J. Chem. Technol. Biotechnol. 74, 256–263.

Klatt, K.U., Marquardt, W., 2009. Perspectives for process systems engineering—personal views from academia and industry. Comput. Chem. Eng. 33, 536–550.

Mathias, P.M., 2014. Some examples of the contribution of applied thermodynamics to post-combustion CO_2-capture technology. Fluid Phase Equilib. 362, 102–107.

Mistry, S.L., Kaul, A., Merchuk, J.C., Asenjo, J.A., 1996. Mathematical modelling and computer simulation of aqueous two-phase continuous protein extraction. J. Chromatogr. A 741, 151–163.

Mündges, J., Zierow, J., Zeiner, T., 2015. Experiment and simulation of an aqueous two-phase extraction process for the purification of a monoclonal antibody. Chem. Eng. Process. Process Intensif. 95, 31–42.

OriginLab 2012. OriginLab, Northampton, MA. 8.6 ed.

Pollock, J., Ho, S.V., Farid, S.S., 2013. Fed-batch and perfusion culture processes: economic, environmental, and operational feasibility under uncertainty. Biotechnol. Bioeng. 110, 206–219.

Prinz, A., Koch, K., Gorak, A., Zeiner, T., 2014. Multi-stage laccase extraction and separation using aqueous two-phase systems: experiment and model. Process Biochem. 49, 1020–1031.

Process Systems Enterprise 2017. gPROMS.

Reschke, T., Brandenbusch, C., Sadowski, G., 2014. Modeling aqueous two-phase systems: I. Polyethylene glycol and inorganic salts as ATPS former. Fluid Phase Equilib. 368, 91–103.

Rito-Palomares, M., 2004. Practical application of aqueous two-phase partition to process development for the recovery of biological products. J. Chromatogr. B: Anal. Technol. Biomed. Life Sci. 807, 3–11.

Rosa, P.a.J., Azevedo, A.M., Sommerfeld, S., Mutter, M., Aires-Barros, M.R., Backer, W., 2009. Application of aqueous two-phase systems to antibody purification: a multi-stage approach. J. Biotechnol. 139, 306–313.

Samatou, J.A., 2012. Modelling and Simulation of Antibody Purification by Aqueous Two-phase Extraction. Technischen Universität Dortmund.

Samatou, J.A., Wentink, A.E., Rosa, P.a.J., Azevedo, A.M., Aires-Barros, M.R., Backer, W., Gorak, A., 2007. Modeling of counter current monoclonal antibody extraction using aqueous two-phase systems. 17th European Symposium on Computer Aided Process Engineering 24, 935–940.

Simon, L., Gautam, S., 2004. Modeling continuous aqueous two-phase systems for control purposes. J. Chromatogr. A 1043, 135–147.

Soares, R.R., Azevedo, A.M., Van Alstine, J.M., Aires-Barros, M.R., 2015. Partitioning in aqueous two-phase systems: analysis of strengths, weaknesses, opportunities and threats. Biotechnol. J. 10, 1158–1169.

Tubio, G., Nerli, B., Pico, G., 2007. Partitioning features of bovine trypsin and alpha-chymotrypsin in polyethyleneglycol–sodium citrate aqueous two-phase systems. J. Chromatogr. B: Anal. Technol. Biomed. Life Sci. 852, 244–249.

Tulsyan, A., Forbes, J.F., Huang, B.A., 2012. Designing priors for robust Bayesian optimal experimental design. J. Process Control 22, 450–462.

Valente, K.N., Lenhoff, A.M., Lee, K.H., 2015. Expression of difficult-to-remove host cell protein impurities during extended chinese hamster ovary cell culture and their impact on continuous bioprocessing. Biotechnol. Bioeng. 112, 1232–1242.

Zafarani-Moattar, M.T., Sadeghi, R., 2001. Liquid–liquid equilibria of aqueous two-phase systems containing polyethylene glycol and sodium dihydrogen phosphate or disodium hydrogen phosphate — experiment and correlation. Fluid Phase Equilib. 181, 95–112.